Advances in Bioresearch
Adv. Biores., Special Issue 1: 2023: 415-434
©2023 Society of Education, India
Print ISSN 0976-4585; Online ISSN 2277-1573
Journal's URL:http://www.soeagra.com/abr.html
CODEN: ABRDC3
DOI: 10.15515/abr.0976-4585.S1.415534

Advances in Bioresearch

In Silico Analysis of Bioactive Phytocompounds as Inhibitors of Penicillin-Binding Protein 2a (PBP2a) and Class A Beta-Lactamase of Target Microorganisms

Milan Dabhi[1], Gibson A. Sabuholo[1], Gargi H. Sharma[1], Jayvi K. Patel[1], Dweipayan Goswami[1*]
Department of Microbiology & Biotechnology, School of Science, Gujarat University, Ahmedabad-380009 Gujarat, India
Milan Dabhi (ORCID: 0000-0001-6581-8389)
Dweipayan Goswami (ORCID: 0000-0003-0165-0294)
Details of correspondence
Email: dweipayan.goswami@gujaratuniversity.ac.in; dweipayan.guresearch@gmail.com

ABSTRACT
*Antimicrobial resistance (AMR) of pathogenic bacteria to Beta-lactam antibiotics is one of the most serious global public health threats. The greatest concern is the development of new effective therapeutics to combat these resistant pathogens. Plant-derived antimicrobial agents have recently piqued researchers' interest. In this study, molecular docking for 553 bioactive phytocompounds against PBP2a (PDB ID: 3ZFZ and 4DKI) and class A beta-lactamase (PDB ID: 6NVU and 4ZBE) was performed in Linux using UCSF Chimera, Open Babel, and AutoDock Vina, to unmask the potential inhibitors. Phytocompounds with higher binding energies (kcal mol^{-1}) to these receptor proteins were selected for post-docking analysis using BIOVIA Discovery Studio 2021 Visualizer. This study resulted in top 7, 10, 8, and 8 phytocompounds with higher binding energies and formation of hydrogen bonds interactions with key amino acids of the active sites including SER403 for 3ZFZ and 4DKI, SER237, SER70 for 6NVU and SER69 for 4ZBE respectively. Rutin (**1**) and 3,3'-Biplumbagin (**13**) were top best screened-out phytocompounds that exhibited the highest binding energies and good interactions with MRSA's Penicillin-Binding Protein 2a (PBP2a) and class A beta-lactamase of E. coli and K. pneumonia. This suggests that these compounds may be considered as potential drug candidates for the designing and development of new drugs to treat different human bacterial infections exhibiting beta-lactam antibiotics resistance. Nevertheless, molecular dynamics and simulation, in vitro, and in vivo study validations are needed.*

KEYWORDS: *Penicillin-binding protein-2a; Class A Beta-lactamase; Phytochemicals; Molecular docking; Methicillin-resistances staphylococcus aureus (MRSA); Klebsiella pneumoniae.*

Received 29.05.2023 Revised 26.07.2023 Accepted 13.08.2023

How to cite this article:
Milan D, Gibson A. S, Gargi H. S, Jayvi K. P, Dweipayan G. *In Silico* Analysis of Bioactive Phytocompounds as Inhibitors of Penicillin-Binding Protein 2a (PBP2a) and Class A Beta-Lactamase of Target Microorganisms. .Adv. Biores., Special 1:2023: 415-434.

INTRODUCTION

Antimicrobial resistance (AMR) of pathogenic bacteria to conventional antibiotics is one of the most serious global public health threats [1]. Bacterial resistance to antibiotics is either through the activation of efflux pumps, destruction and modification of antibiotic compounds through enzymes, or mutations that occur on the microbial target proteins resulting in the loss of affinity by the antibiotics [2, 3]. The discovery of antibiotics helped to treat different infectious diseases caused by pathogenic bacteria. The first discovered antibiotic was penicillin (a beta-lactam antibiotic) in 1928 by a Scottish physician and microbiologist, Sir Alexander Fleming, and pure penicillin was used for treatment in 1941 when it saved many victims of World War II. In within 2 years following the introduction and use of penicillin to treat clinical Staphylococci bacterial diseases, bacteria developed a resistance mechanism to overcome its activity [4–6] with the resistance mechanism conferred by beta-lactamase enzymes (penicillinase) production that works by hydrolysing the beta-lactam ring of penicillin antibiotics (A. Bondi, C. Dietz, 1945). In 1960 methicillin, a semi-synthetic penicillin derivative was introduced in clinical use and was effective in binding covalently to Penicillin-Binding Proteins (PBPs) and could not be easily metabolized by penicillinase. Shortly after its introduction, methicillin-resistance cases were reported in the United Kingdom. Bacteria evolved a

surrogate transpeptidase via Penicillin-Binding Protein 2a (PBP2a) [8] that did not interact with methicillin for acylation because of its low binding affinity to beta-lactam ring, thus this PBP catalyses transpeptidation activity to allow cell wall synthesis at the presences of beta-lactams [9].

Penicillin-Binding Proteins (PBPs) are group of transpeptidase enzymes responsible for bacterial cell wall biosynthesis by catalysing the cross-linkage between peptidoglycans by recognizing the acyl-D-Ala-D-Ala moiety as the native substrate for this cross-linkage reaction (Sun Song et al., 2014). Beta-lactam antibiotics which are the core structure for all penicillin-like antibiotics are commonly used against bacteria pathogens by inhibiting PBPs catalytic activity and block the processes of cell wall biosynthesis. This is because of the structural similarity between acyl-D-Ala-D-Ala moiety and beta-lactam ring (Donald J. Tipper and Jack L. Strominger, 1966), the latter can bind covalently to transpeptidase active site and irreversibly inhibit the catalytic activity of the active site [12]. Therefore, beta-lactams and other penicillin-like antibiotics inhibit and kill bacteria by blocking their cell wall synthesis. PBPs are ubiquitously expressed in gram-positive bacteria. Both susceptible and resistant strains of *S. aureus* produce five major PBPs; PBP1, PBP2, PBP3, PBP4, and PBP5 (Nicholus A. Turner et al., 2020). However, methicillin-resistant *S. aureus* (MRSA) has the potential to express PBP2a, the most alarming modified PBPs that confers resistance to penicillin and cephalosporin class of antibiotics (Kim et al., 2012; Gian Maria et al., 2016). The resistance gene for methicillin resistance in MRSA strains is due to the acquisition of the *mecA* gene through horizontal gene transfer [8, 16], and *mec A* is highly conserved and distributed among clinical MRSA isolates (>90% sequence identity between strains) [8, 17].

Beta-lactamases are diverse class of enzymes produced by bacteria that break open the beta-lactam ring, inactivating the beta-lactam antibiotic. Some beta-lactamases are encoded on mobile genetic elements (e.g. plasmids); others are encoded on chromosomes. Beta-lactamase production is among the most clinically important mechanisms of resistance for gram-negative bacterial pathogens. Understanding the most common types of beta-lactamases produced by different pathogens can help with susceptibility interpretation, therapeutic decision-making, and infection control practices [18, 19]**.** Enterobacteriaceae (*Citrobacter, Escherichia coli, Klebsiella pneumoniae, Proteus vulgaris, Salmonella, Shigella),* are common bacteria treated by beta-lactamase inhibitors. Additionally, beta-lactamase is also present in gram-positive bacteria such as *Staphylococcus aureus* [20]. However, beta-lactamase inhibitors are less commonly used for the treatment of *staphylococcus aureus* due to the presence of an alternate resistance mechanism by Penicillin-Binding Proteins (PBPs) which is ubiquitous among gram-positive bacteria. Beta-lactamase inhibitors work by one of two primary mechanisms. They may become substrates that bind the beta-lactamase enzyme with high affinity but form sterically unfavourable interactions, such as the acyl-enzyme. They may also act as "suicide inhibitors," which permanently inactivate the enzyme through secondary chemical reactions in the active site [20].

The use of various classes of antibiotics since the first discovery led to the emergence of multidrug-resistant (MDR) strains [16], thus the management of multi-drug resistant strains of *S. aureus, K. pneumonia* has become increasingly difficult due to its resistance to beta-lactam antibiotics and other classes of antibiotics by producing excessive beta-lactamases and/or by expressing low affinity PBPs. Therefore, there no doubt that there is a pressing need to identify, design and develop new safe and effective drug molecules for treating beta-lactam resistant bacteria strains by inhibiting the activity of beta-lactamase enzymes and Penicillin-Binding protein 2a (PBP2a).

Detailed studies for better understanding the interactions of beta-lactam antibiotics and bet lactamase inhibitors with their respective target receptor proteins have been conducted at molecular levels and the findings have been used as a reference in searching for new and effective inhibitors of those proteins from natural and synthetic products [21]. Plant extracts have been used for many years to cure different diseases [22, 23], hence medicinal plants are considered a significant source for discovering new molecules with potential therapeutic activities. In India, they have been using medicinal plants for more than 5,000 years now in the indigenous system of medicine such as Ayurveda, Unani, Siddha, homeopathy, and naturopathy [24, 25]. The significances of medicinal plants as interesting sources for new safe and effective antibiotic molecules are because they have developed complex-defensive mechanisms against invading microorganisms such as by secretion of secondary metabolites and their rich chemo-diversity across approximately 381,000 species of global plants [26] (http://www.worldfloraonline.org/). The proven safety and clinical effectiveness of medicinal plant extract in day-to-day practices of traditional medicines across the world [27], their ease of availability [28], and the potential to act synergistically with other bioactive compounds [29] make them significant sources for effective new drug molecules.

There are many study reports on *in vitro* studies of phytochemicals, that suggest that phytochemicals and their components as natural plant products can be used as anti-MRSA agents if properly researched [30]. For instance, when terpinen-4-ol (TTO) was used alone for 6 days, shows a fourfold increase in S. aureus

MIC values [31]. Despite that there is an abundance of *in vitro* studies on the antimicrobial activity of phytochemicals, results for their mechanisms of action (MoA) are still limited and only a few studies have been published. Goel et al., reported the inhibition of PBP2a from MRSA using usnic acid which was extracted from fruticose lichen *Ramalina roesleri* of Himalaya mountain [32], in this study usnic acid exhibited inhibitory capacity higher than oxacillin. Maulana, reported curcumin, germacrone, and zerumbone from rhizome herbal plants; Turmeric (*Curcuma lon,ga*) and Bitter Ginger (*Zingiber zerumbet*) as promising inhibitors penicillin-binding proteins in MRSA [33]. Lakshmi et al., conducted a study on *S. aureus* beta-lactamase inhibition using 15 polyphenol phyto-ligands in which kaempferol from *Laurus nobilis* (Lauraceae) exhibited a higher inhibitory capacity against MRSA [34]. Mohamed et al., performed an in silico analysis for inhibition of PBP2a of MRSA SO-1977 isolated from Sudan, in this study the docked compounds reported to have demonstrated good binding affinities with hydrogen bond interactions to Ser404 which is an important binding site residue for beta-lactams activity [35]. Santiago et al., reported in vitro synergistic inhibition of MRSA by a combination of *Duabanga grandiflora* fractional extract with ampicillin in which MIC of ampicillin against MRSA was reduced to 0.78 mg/L (64-fold) from initial value of 50 mg/L. The synergistic inhibition activity of PBP2a of MRSA grown culture was elucidated ua sing western blot assay in which no PBP2a band was identified [36]. Therefore, the present study is going to explore the inhibition affinities and ligand interactions of different reported anti-microbial phytocompounds to PBP2a of MRSA and class A beta-lactamase enzymes of *E. coli*; and *K. pneumonia* strain using molecular docking analysis, one of the most important modelling tools in modern drug discovery.
MD stands for Molecular Dynamic simulation is very essential for evaluating binding stability of lead ligand to target protein. MD is computational approach to evaluate motion of macromolecules, ions and water. It aids in identifying best bounded compound. Through MD simulation, the stability of interaction between protein and ligand is analysed. This interaction types are categorized into four types: Hydrogen Bonds, Hydrophobic interactions, Ionic contacts and Water Bridges. During MD assessment, the RMSD that stands for Root mean square deviation examination is of very important to compute for evaluating the typical change in movement of the structural atoms with respect to the reference starting frame. The position of docked ligand with protein in the complex is set as the initial reference orientation and afterward the changes taking place during MD simulation is checked by overlapping all the protein movement frames obtained. Using Desmond package, MD simulation of reference native ligands and top best compound; rutin, were performed for 3ZFZ, 4DKI and 6NVU.

MATERIAL AND METHODS

META DATA ANALYSIS AND LIGANDS PREPARATION

A meta-data analysis of the phytochemicals that having antimicrobial activity was conducted by analysing data from previously published studies. A total of 553 names of phytochemical compounds from different medicinal plants and their information were collected mainly from PubMed, IMPPAT (Indian medicinal plants, phytochemistry, and therapeutics), Current contents, Biosis previews, and Web of Science and from peer-reviewed journals. The database included phytochemicals and their sources, mode of action, classification, and whether *in-silico* work is done or not. Generally, the classification of phytochemicals was based on their structures and categorized into major groups of alkaloids, tannins, carbohydrates, glycosides, terpenoids, polyphenols, flavonoids, and steroids. The 3D structures of the phytochemicals were retrieved in SDF format from NCBI-PubChem. Ligands were energy minimized using Obminimize force field MMFF94, and converted into pdbqt files using Open Babel [37].

RECEPTOR PROTEINS PREPARATION

The crystal structures of Penicillin-Binding Protein 2a (PBP2a) from MRSA, PDB ID: 4DKI; resolution 2.90Å, PDB ID: 3ZFZ; resolution 2.25Å, and of class A beta-lactamase enzymes from *Escherichia coli and Klebsiella pneumonia*, PDB ID: 6NVU; resolution 2.50Å, and PDB ID: 4ZBE; resolution 1.80Å were selected as receptor proteins, and their 3D structures were downloaded from the RCSB Protein Data Bank (http://www.rcsb.org). Using Dock Prep Tool of UCSF Chimera 1.16, receptor proteins were prepared for docking, by removing interferences such as co-crystallized ligands, water molecules, and other bound ligands. The grid coordinates were computed around the ligand binding site in the receptor protein structure using the AutoDock Vina. Grid-boxes were created in such a way that covers the entire protein binding site and accommodates the ligands to move freely in it. The force field Gasteiger was used to add hydrogen and calculation of net charges.

MOLECULAR DOCKING

The binding affinities and types of interaction were studied using molecular docking analysis. UCSF-Chimera 1.16 [38] was used for redocking of native co-crystallized ligands (references ligands) in the receptor proteins. The output files "Docking.receptor.pdbqt" were used for receptor proteins-

phytocompounds docking calculations performed by an automated docking tool; AutoDock Vina v1.2.3 in Linux by running Vina perl script command line (Vina_linux.pl). AutoDock Vina is an open-source software tool widely used for molecular docking [39]. All the used codes and commands for multiple ligands docking in Vina was retrieved from free available online repository at (https://github.com/DweipayanG). Molecular Docking results were the created files in the working folders in the form of ''out.pdbqt''.

PROTEIN-LIGAND INTERACTION ANALYSIS

Analysis and visualization of the ligand and receptor interactions were carried out using Biovia Discovery Studio 2021 Visualizer. Both 2D and 3D protein-ligand interactions were visualized from docking output files by first loading and open the pdbqt output file with different ligand binding poses in UCSF Chimera. Each pose was analysed and saved in PDB format. All the saved poses were opened and viewed under the Receptor-Ligand Interaction platform of Discovery Studio Visualizer. The best binding pose was identified based on binding score in (kcal mol-1) of ligand to receptor protein and the key active site's amino acids involved in the ligand recruitment by comparing with docking results of reference ligand. Types of binding interactions between ligand and receptor protein were analysed in 2D structures of the visualizations. The amino acids of the target receptor protein involved in the binding interactions of the best binding pose of the ligand were also analysed.

MOLECULAR DYNAMICS AND SIMULATION

The molecular dynamics and simulations for top best complex 4DKI-rutin, 3ZFZ-rutin, and 6NVU-rutin together with reference docked complex of 4DKI-ceftobiprole, and 6NVU-clavulanic acid were performed for a period of 10 ns for each of the docked complex using Desmond package [40]. The TIP3P solvent model was used to build the system, and it specifies a 3-site rigid water molecule with charges and Lennard-Jones parameters given to each of the atoms. To set up the periodic boundary conditions (PBC), an orthorhombic shape simulation box with dimensions of 10 Å x 10 Å x 10 Å was selected, along with default box angles and box volume (Å3). Using OPLS2005 force fields, neutralization was then performed by adding 3 Na+ ions and a salt concentration of 0.15 M Na+ and Cl counter ions to simulate the background salt and physiological conditions. After the system is incorporated, it was minimized with restraints using Steepest Descent Energy Minimization with NPT (constant Number of Particles, Pressure, and Temperature), 300 K temperature, and 1.013 bar atomic pressure and default surface tension using Smooth Particle Mesh Ewald (PME) method to neutralize the electrostatic interactions. For each of the complexes, the MD simulation was run for a duration of 10 ns, with energy recording intervals of 1.2 ps and trajectory recording intervals of 4.8 ps. The Simulation Interaction Diagram wizard was used, which computes trajectories for Root Mean Square Deviation (RMSD) and Root Mean Square Fluctuation (RMSF), to analyze each trajectory. In addition, with respect to a 10 ns simulation, protein-ligand contact profiles for essential interacting amino acid residues and timelines of these specific interactions are also computed [41]

RESULTS

MOLECULAR DOCKING ANALYSIS

In the present study molecular docking analysis was performed to analyse the binding affinities and ligand interactions of the prepared metadata of 553 bioactive phytocompounds and co-crystallized ligands (reference ligands); ceftaroline, ceftobiprole, clavulanic acid and avibactam to active sites of PBP2a (3ZFZ and 4DKI) and Beta-lactamases (6NVU and 4ZBE). Ligand binding energy calculations were performed by AutoDock Vina and protein-ligand complex binding interactions were analysed and visualized using Discovery Studio 2021 Visualizer. Docking results of the phytocompounds with each receptor protein were analysed and compared with docking results of reference ligands. Variations in binding affinities and interactions of phytocompounds and reference ligands with receptor proteins were observed and analysed. Screening out of best protein-phytocompound complex was based on two criteria; First, the exhibited binding affinities (Dock scores in kcal/mol) by the ligand towards the active site of receptor protein in comparison to that exhibited by reference ligand. A phytocompound possessed higher binding affinities than that of reference ligand was considered as the best hit (the more negative value the better binding affinity). Second, the formation of hydrogen bond(s) interaction between phytocompound and the key amino acids of the protein active site i.e. Ser403 for PBP2a (3ZFZ and 4DKI), Ser69 for 4ZBE, Ser70 and Ser237 for 6NVU.

ANALYSIS OF 3ZFZ-PHYTOCOMPOUND COMPLEXES

The prepared metadata of phytocompounds was screened against PBP2a; 3ZFZ, to search for the best protein inhibitor using ceftaroline a beta-lactam antibiotic as reference ligand. Docking results of ceftaroline against 3ZFZ exhibited the binding energy of -8.65 kcal mol^{-1} with the formation of seven hydrogen bonds interaction with active site's amino acids which are Lys406, Ser403, Asn464, Glu602, Ser462, Gly520, and Thr600 of which Ser403 is a key amino acid that form the active site of PBP2a, 3ZFZ,

(Table 1 and Figure 1A) [42]. All the 3ZFZ-phytocompound complexes obtained as dock outputs were analysed using ceftaroline docking results as a reference. After analysis of all the complexes; on the basis of the Dock scores, out of the 553 screened phytocompounds, a total of top 7 compounds (Rutin, 3, 4', 7-Trihydroxyflavone-7-O-rutinoside, Isoquercetrin, Isoquercitrin, Tiliroside, Theaflavine and 2-(3,4-dihydroxy phenyl)-ethyl-O-β-D-glucopyranoside) were found to exhibit higher binding energies with the formation of more hydrogen bonds interaction with amino acids of the active site of 3ZFZ than ceftaroline (Table 1). Among the top 7 compounds, rutin (**1**) found to exhibit the highest binding energy -13. 89 kcal mol^{-1} with the formation of twelve (12) hydrogen bonds interaction (Figure 1A-left) in the active site pocket of 3ZFZ than all other top compounds (Table 1).

ANALYSIS OF 4DKI-PHYTOCOMPOUND COMPLEXES

PBP2a; 4DKI, is co-crystallized with ceftobiprole a beta-lactam antibiotic in the active site. The prepared metadata of 553 bioactive phytocompounds was docked against 4DKI to screen out potential PBP2a inhibitor using ceftobiprole as reference ligand. Docking results of ceftobiprole against 4DKI showed that ceftobiprole exhibited -8.9 kcal mol^{-1} binding energy with the formation of eight (8) hydrogen bonds interaction between Ser403, Thr600 (3 H-bonds), Ser598, Asn464, Gln521, and Glu602 in the active site of receptor protein; 4DKI, of which Ser403 is a key amino acid that form the active binding site of 4DKI (Table 2 and Figure 1B) [43]. All 4DKI-phytocompound complexes formed from docking processes were analysed and visualized in comparison with reference ceftobiprole docking results. After analysis of all the docked 4DKI-phytocompound complexes; on the basis of the Dock score, among the 553 phytocompounds docked, the top 10 compounds (Rutin, Isoquercetrin, 3,4',7 Trihydroxyflavone-7-O-Rutinoside, Corilagin, Tiliroside, Isoquercetin, 2-(3,4-dihydroxyphenyl)-ethyl-O-beta-D-glucopyranoside, Epigallocatechin Gallate, Theaflavine, Chlorogenic acid) were found to possess higher binding energies towards the active site of 4DKI than ceftobiprole (Table 2). Out of this top 10 compounds, six compounds found to form more hydrogen bonds interaction between amino acids in the active site of 4DKI i.e. Rutin (9 H-bonds), Isoquercetrin (13 H-bonds), 3,4',7 Trihydroxyflavone-7-O- Rutinoside (10 H-bonds), Corilagin (11 H-bonds), 2-(3,4-dihydroxyphenyl)-ethyl-O-beta-D-glucopyranoside (10 H-bonds), and Chlorogenic acid (10 H-bonds) than ceftobiprole that formed 8 H-bonds. Four compounds; Tiliroside (7 H-bonds), Isoquercetin (7 H-bonds), Epigallocatechin Gallate (6 H-bonds), and Theaflavine (6 H-bonds) formed less number of hydrogen bonds in the active site of 4DKI (Table 2). Rutin (**1**) was found to be the top best ligand by having the highest binding energy -12.6kcal mol^{-1} to 4DKI than all the other top compounds as compared to reference ceftobiprole with -8.9 kcal mol^{-1} (Table 2).

ANALYSIS OF 6NVU-PHYTOCOMPOUNDS COMPLEXES

In this study, two class A beta lactamase enzyme proteins were selected. One of theproteinsn was 6NVU from beta-lactam resistant *E. coli* strain, this is available in PDB database in complex with beta-lactamase inhibitor; clavulanic acid. Analysis of docking results of the 6NVU-clavulanic acid complex showed that clavulanic acid has binding energy of -6.2 kcal mol^{-1} towards 6NVU binding site pocket with the ability to form five (5) hydrogen bonds interaction with amino acids; Ser70, Ser237, Ser130 (2 H-bonds), and Thr235 of which Ser70 and Ser237 are key amino acids that form the active site of 6NVU (Table 3 and Figure 1C) [44]. These compounds exhibited inhibitory effects to 6NVU with higher binding energies than that exhibited by reference clavulanic acid inhibitor (-6.2 kcal mol^{-1}) (Table 3). Furthermore, among these compounds, two compoundhavethe as ability to form more hydrogen bonds interaction i.e. 2-(3, 4-dihydroxyphenyl)-ethyl-O- beta-D-glucopyranoside and Isoquercetrin each formed six (6) H-bonds with the active site's amino acids of the 6NVU while Chlorogenic acid formed less (three) hydrogen bonds interaction (Table 3). Among the screened-out top 8 compounds, rutin (**1**) was found to be the top best inhibitor by exhibiting the highest binding affinity -10.54 kcal mol^{-1} to 6NVU than all the top compounds as compared to reference clavulanic acid with -6.2 kcal mol^{-1} (Table 3).

ANALYSIS OF 4ZBE-PHYTOCOMPOUNDS COMPLEXES

A beta-lactamase enzyme; 4ZBE, from beta-lactam resistant *K. pneumonia* strain was selected, this protein is available in Protein Data Bank (PDB) database in complex with beta-lactamase inhibitor; avibactam, [45]. From the analysis of docking results of the 4ZBE-avibactam complex it was observed that avibactam has binding energy of -6.7 kcal mol^{-1} to 4ZBE active site with the formation of seven (7) hydrogen bonds interaction with amino acids; Ser69 (2 H-bonds), Thr236 (2 H-bonds), Thr234, and Asn131 (2 H-bonds) of which Ser69 is a key amino acid that form the active binding site of 4ZBE (Table 4 and Figure 1D) [45]. Eight (8) compounds (3, 3-biplumbagin, curcumin, rosmarinic acid, rutin, Aegilinol, 2-(3, 4-dihydroxyphenyl) ethyl-O- beta-D-glucopyranoside, chlorogenic acid, melanoxetin, N-formimidoyl thienamycine) were screened-out as the top inhibitors of beta-lactamase; 4ZBE, from the metadata of 553 phytocomounds.

These compounds exhibited binding energies to 4ZBE's active site higher than that exhibited by avibactam inhibitor (-6.7 kcal mol^{-1}) (Table 4). Out of these top 8 compounds screened-out against 4ZBE, 3, 3-bi-plumbagin (**13**) was found to be the top best by having the highest binding energy -12.59 kcal mol^{-1} towards 4ZBE than all other top compounds as compared to reference avibactam with -6.7 kcal mol^{-1}. However, on the basis of interacting amino acid residues, 3, 3-biplumbagin was able to form hydrogen bonds interaction with 4ZBE less to that formed by avibactam (Table 4).

MD SIMULATION ANALYSIS

In order to determine the stability and validate the docking data of the proteins complex in the presence of rutin, 4DKI-rutin, 3ZFZ-rutin, and 6NVU-rutin together with 4DKI-ceftobiprole, and 6NVU-clavulanic acid were subjected to MD simulation over a period of 10ns. RMSD, RMSF, and protein-ligand contacts were computed and analysed.

RMSD ANALYSIS

In analysing the stability of Molecular dynamics simulation trajectories, RMSD is considered as a fundamental parameter. The RMSD was plotted as a function of time at x-axis and deviations of protein's backbone atoms (lefts limb) and ligand atoms (right limb) at Y-axis to analyse the stability of each complex system under study throughout the simulation period.

RMSF ANALYSIS

The protein's RMSF value give information about the fluctuation behaviour of residues of a simulated protein in aqueous system with respect to its initial position. Commonly, the protein tails (N- and C-terminal) fluctuate more than other inside residues of the protein. In the RMSF figures, the up and down peaks show different residues of the protein that fluctuate throughout the simulation course. Alpha-helical and beta-strand regions which are inflexible are indicated in red and blue colours respectively. The interacting residues, marked in green colour bars are somehow less fluctuating, they are stable. In general, the high RMSF value suggests more flexibility while low RMSF suggests limited flexibility of a residue, with respect to its initial position.

PROTEIN-LIGAND CONTACT ANALYSIS

For all the ligands (references and rutin), most of ligand interactions with protein residues which were identified in the docking results analysis are validated and observed in molecular dynamics and simulation trajectories. The stable protein-ligand interactions are observed throughout the simulation period. Most of the interactions are classified into main four types, Hydrophobic interactions, Hydrogen Bonds, Ionic interactions and Water Bridges. In the protein-ligand contact figures, the compounded vertical bars indicating the interaction type between protein residue (X-axis) and ligand and the interaction fraction (Y-axis). These stacked bar charts are normalized over the course of the simulation: For example, a value of 0.6 (at Y-axis) suggests that 60% of the simulation time the specific type interaction was maintained. Also, in a situation where protein residue makes multiple interactions of the same subtype with the ligand, the fraction values >1.0 are possible.

PBP2A-4DKI

For the docked complex of 4DKI-ceftabiprole it was observed that the protein's RMSD value (Figure 2A-left limb) deviated from 1.6 Å fixed point and peaks up to 6.4 Å at 4 to 6 ns then converges to 4.8 Å at the end of simulation, while Ligand's RSMD value (right limb) was almost fixed at 1.4 Å throughout. The value for 'Lig fit Prot' in this complex found to deviate below in the same fashion, parallel, close to protein backbone value throughout the simulation. For 4DKI-rutin complex, protein's RMSD value (Figure 2B-left limb) didn't exceed 4.8 Å; has fixed point at 1.2 Å, peaks up to 4.8 at 2 ns and then was maintained between 2.4 Å to 4.2 Å, finally converges to 3.6Å at the end of simulation, while the ligand's RMSD value (right limb) was maintained between 0.6 to 0.8 Å throughout the simulation. It's RMSD for 'Lig fit Prot' was initially in contact with protein backbone up to 2 ns, then moved below in parallel fashion to protein backbone. RMSF values of all complexes of 4DKI (Figure 3A and B) was observed initially to be high, but they were less thereafter for most interacting residues which shows fluctuation values below 2.7 Å. The patterns for the values of RMSF and B-factors were also consensus aligning. Predicting that all the protein–ligand complexes have less changes, inferring a lesser flexing of protein backbone residues. For protein-ligand contact in PBP2a-4DKI complexes all the normal interacting residues with ceftobiprole and rutin were observed. Amino acids Ser403, Thr600, Ser598, Lys 597 and Ser462 are all portrayed in which Ser403 is a key active site residue. For a complex of 4DKI-ceftobiprole (Figure 4A), the reported inhibition interaction fraction value of ceftobiprole to Ser403 was nearing 2.0 (~200%), while the reported inhibition fraction value of rutin to Ser403 in the 4DKI-rutin complex was less around 0.6 (~60%) (Figure 4B). Figure 5 are the timeline representations of the respective residues interaction and contacts (hydrogen bonds, hydrophobic contacts, Ionic contacts, and Water bridges) for PBP2a-4DKI complexes. All interacting amino acids with

the ligands are depicted, for those amino acids with more than one interaction of same type are indicated by a darker shade of orange as it is explained by the vertical scale on the right side of the plot.

Beta-lactamase-6NVU

In the (Figure 6A) it was observed that the RSMD value of the protein's backbone atoms (left limb) for 6NVU-clavulanic acid complex has 0.6 Å reference point and its deviation was maintained between 1 Å to 1.3 Å throughout the simulations period. The RMSD value for ligand's atoms (right limb) peaks up to 1.6 Å in between 0.8-4 ns, then was maintained around 0.8 Å till end of simulation. It's RMSD for 'Lig fit Prot,' initially observed to deviate far above the protein backbone, then from 4 ns it was in close contact with protein backbone throughout the simulation (0.8 Å to 1.3 Å). The RMSD value of protein's backbone in the 6NVU-rutin complex (Figure 6B-left limb) was observed to deviate continuously from fixed point 0.8 to 1.6 Å throughout the simulation, while the Ligand RMSD value ('Lig fit Lig'-right limb) didn't exceed 3.0 Å. 'Lig fit Prot' RMSD value observed to deviated far above the protein backbone up to 2.4 Å at the end of simulation process. RMSF values in all complexes of 6NVU, were observed to be low around 0.8 Å and below for most of interacting residues of the protein (Figure 7A and B). The B-factors value were in agreement with RMSF values, in which B-factors were below 45%. The reported protein-ligand interaction fraction values of clavulanic acid to key Ser70 and Ser237 were 0.6 (˜60%) and 1.25 (˜125%) respectively (Figure 8A) while for rutin, the reported value on Ser70 was below 10%, and nearly to 200% for Ser237 (Figure 8B). The timeline representation of the respective residues interaction and contacts (hydrogen bonds, hydrophobic contacts, Ionic contacts, and Water bridges) of this protein complexes are shown in the figure 9. In which, all the interacting amino acids with the ligands are depicted, for those amino acids with more than one interaction of same type are indicated by a darker shade of orange.

PBP2a-3ZFZ

The RMSD value of the protein backbone in the 3ZFZ-rutin complex was observed to move continuously from fixed point 1.6 Å to 6.4 Å then back to 3. 2 Å at 5.8 ns then moved up to 5.6 Å at the end of simulation (Figure 10A-left limb). The ligand RMSD value ('Lig fit Lig'-right limb) for this complex was observed to deviate from fixed point 0.8 Å and maintained between 1.2 Å to 2 Å from 0.8 ns to 10 ns of the simulation process. At the same time, the RMSD value for 'Lig fit Prot' deviated in the same fashion parallel to protein backbone. At around 8 ns it was deviated below the protein RMSD, finally it converges at the value below the protein backbone (4.8 Å) at the end of 10 ns simulation period. In figure 10B, the RMSF values initially was high, but was less thereafter for most interacting residues which shows to fluctuate below 2.7 Å. The patterns for the RMSF values and B-factors were consensus aligning. Predicting that the protein–ligand complex has less changes, inferring a lesser flexing of protein backbone residues. In the protein-ligand contact (Figure 11A), all the normal interacting residues; Ser403, Thr600, Ser598, Lys 597 and Ser462 are depicted and Ser403 is a key active site residue. For this complex, the reported interaction fraction value of rutin to Ser403 was nearly 0.65 (˜65%). A timeline representation of the respective residues interaction and contacts (hydrogen bonds, hydrophobic contacts, Ionic contacts, and Water bridges) for 3ZFZ-rutin complex is shown in the figure 11B, in which all interacting amino acids are depicted. For those amino acids with more than one interaction of the same type are indicated by a darker shade of orange as it is explained by the vertical scale on the right side of the plot.

Table 1 Details of binding energies and hydrogen bonds interaction of top 7 phytocompounds and reference antibiotic; ceftaroline, to MRSA's PBP2a (PDB ID: 3ZFZ)

Ligand with PubChem CID	Binding Energy (kcal mol^{-1})	Interacting Amino acids Residues	Number of Hydrogen Bonds
Ceftaroline (CID: 9852981) [a]	-8.65	LYS406, SER403, ASN464, GLU602, SER462, GLY520, THR600	7
Rutin (CID: 5280805)	-13.89	SER403, GLN521, ASN464 (2), GLU602, SER462 (2), THR444 (3), GLY520, THR600	12
3,4',7-Trihydroxyflavone-7-O-rutinoside (CID: 101422354)	-13.38	SER403, ASN464 (2), GLU602, SER463, GLN613, SER462, THR600	8
Isoquercetrin (CID: 5480505)	-13.15	SER403, GLN521 (2), SER462 (2), THR600, GLY520, ALA642, SER598, GLU602 (2)	11
Isoquercitrin (CID: 5280804)	-13.08	SER403, GLN521 (2), ASN464, SER462 (2), THR600, THR444, SER598	9
2-(3,4-dihydroxyphenyl) ethyl-O-β-D-glucopyranoside (CID: 5316821)	-11.71	SER403, GLU602, SER462, GLN521, THR600 (2) SER598	7
Tiliroside (CID: 5320686)	-11.12	SER403, GLU602 (2), GLN521 (2), SER462 (2), ASN464 (2), ALA642, ASN442	11
Theaflavine (CID: 135403798)	-9.74	LYS430, SER403 (2), GLN521 (2), ASN464, ASN464, THR600	8

[a] Reference ligand

Table 2 Details of binding energies (kcal mol^{-1}) and hydrogen bonds interaction of top 10 phytocompounds and reference antibiotic; ceftobiprole, to PBP2a (PDB ID: 4DKI)

Ligands with PubChem CID	Binding Energy (kcal mol^{-1})	Interacting Amino acids Residues	Number of hydrogen bonds
Ceftobiprole (CID: 135413542) [a]	-8.9	SER403, THR600 (3), SER598, ASN464, GLN521, GLU602	8
Rutinn (CID:5280805)	-12.60	SER403, SER462, ASN464, THR600 (2), TYR446, ALA642, SER643 (2)	9
Isoquercetrin (CID: 5480505)	-11.91	SER403 (3), SER462 (4), SER643, THR600, ASN464, TYR446, GLU602, GLN613	13
3,4',7-Trihydroxyflavone-7-O-Rutinoside (CID: 101422354)	-11.08	SER403(2), SER462 (2), THR444, ASN464 (2), GLN521, GLU602 (2)	10
Corilagin (CID: 73568)	-10.75	SER403 (2), SER462 (2), ALA642, ASN464 (3), SER643, TYR446, THR600	11
Tiliroside (CID: 5320686)	-10.63	SER403(2), SER462, ASN464(2), THR600(2), SER642, GLU602, GLN521 (2)	11
Isoquercitrin (CID: 5280804)	-10.53	SER403, SER643, HIS583, ASN464, GLU602, ALA601, GLN613	7
2-(3,4-dihydroxyphenyl)-ethyl-O-β-D-glucopyranoside (CID: 5316821)	-9.97	SER403 (2), SER462 (2), ALA642, ASN464 (2), THR600, SER643 (2)	10
Theaflavine (CID: 135403798)	-9.94	SER403, SER598, HIS583, GLU602, MET641, ALA601	6
Epigallocatechin Gallate (CID: 65064)	-9.95	SER403, SER462, ASN464 (2), THR600 (2), GLU447	7
Chlorogenic acid (CID:179442)	-8.92	SER403 ,SER 589,SER462(4), THR600, SER461 (2), SER400,ASN:464	10

[a] Reference ligand

Table 3 Details of binding energies (kcal mol^{-1}) and hydrogen bond interactions of top 8 phytocompounds and reference inhibitor; clavulanic acid, to beta-lactamase from *E. coli* (PDB ID: 6NVU)

Ligands with PubChem CID	Binding Energy (kcal mol^{-1})	Interacting Amino Acids Residues	Number of Hydrogen Bonds
Clavulanic acid [a]	-6.2	SER70, SER237, SER130 (2), AND THR235	5
Rutin (CID: 5280805)	-10.54	SER70, SER237 (2), THR235 AND ARG220	5
Corillagin (CID: 73568)	-10.21	SER70 (2), SER237, SER130, AND THR235	5
2-(3,4-dihydroxyphenyl)-ethyl-O-β-D-glucopyranoside (CID: 5316821)	-9.12	SER70 (2), SER237 (2), SER130, AND THR235	6
Chlorogenic acid (CID: 1794427)	-9.04	SER70, SER237, AND SER130	3
Isoquercetrin(CID: 5480505)	-8.72	SER70, SER237 (2), THR235 AND ARG220 (2)	6
Isoquercitrin (CID: 5280804)	-8.4	SER70, SER237 (2), SER130, AND THR235	5
3,4',7-Trihydroxyflavone-7-O-rutinoside (CID: 101422354)	-8.05	SER70, SER237 (2), SER130, AND THR235	5
Epigallocatechingallate (CID: 65064)	-7.61	SER70 (2), SER237 (2) AND THR235	5

[a] Reference ligand

Table 4 Details of binding energies (kcal mol^{-1}) and hydrogen bond interactions of top 8 phytocompounds and reference inhibitor; avibactam, to beta-lactamase of *K. pneumoniae* (PDB ID: 4ZBE)

Ligands with PubChem CID	Binding Energy (kcal mol^{-1})	Interacting Amino acids Residues	Number of Hydrogen Bonds

Avibactam [a] (CID: 9835049)	-6.7	SER69 (2), THR236 (2), THR234, AND ASN131 (2)	7
3, 3′-Biplumbagin (CID: 183757)	-12.59	SER69, THR236, THR234 AND ASN131	4
Curcumin (CID: 969516)	-10.9	SER69, THR236, THR234 AND ASN131	4
Rosmarinic acid (CID: 5281792)	-10.3	SER69, SER129 AND THR234	3
Aegelinol (CID: 600671)	-7.95	SER69, SER129 AND THR236	3
2-(3,4-dihydroxyphenyl) ethyl-O-beta-D-glucopyranoside (CID: 5316821)	-7.81	SER69, THR236, THR234 (2) AND SER129	5
Chlorogenic acid (CID: 1794427)	-7.45	SER69, THR236 (2), AND THR234	4
Melanoxetin (CID: 15560442)	-7.39	SER69, THR236, AND THR234	3
N-formimidoyl Thienamycine (CID: 5288621)	-6.97	SER69, THR236, THR234, SER129 AND ASN131	5

[a] Reference ligand

Table 5 Summary of binding Energies (kcal mol^{-1}) of top 16 screened-out phytocompounds and reference antibiotics; ceftaroline, ceftobiprole and inhibitors; clavulanic acid and Avibactam against MRSA's PBP2a (3ZFZ and 4DKI) and Beta-lactamase (6NVU and 4ZBE)

Ligand with PubChem CID		**Binding Energy (kcal mol^{-1})**			
		3ZFZ	**4DKI**	**6NVU**	**4ZBE**
Reference ligand		Ceftaroline -8.65	Ceftobiprole -8.9	Clavulanic acid-6.2	Avibactam -6.7
1	Rutin (CID:5280805)	-13.89	-12.60	-10.54	NP
2	3,4',7-Trihydroxyflavone-7-O-rutinoside (CID: 101422354)	-13.38	-11.08	-8.05	NP
3	3,3′-Biplumbagin (CID: 183757)	NP	NP	NP	-12.59
4	Isoquercetrin (CID: 5480505)	-13.15	-11.91	-8.72	NP
5	Isoquercitrin (CID: 5280804)	-13.08	-10.53	-8.4	NP
6	Corilagin (CID: 73568)	NP	-10.75	-10.21	NP
7	Tiliroside (CID: 5320686)	-11.12	-10.63	NP	NP
8	2-(3, 4-dihydroxy phenyl)-ethyl-O-β-D-glucopyranoside (CID: 5316821)	-11.71	-9.97	-9.12	-7.81
9	Epigallocatechin Gallate (CID: 65064)	NP	-9.95	-7.61	NP
10	Curcumin CID: 969516)	NP	NP	NP	-10.9
11	Rosmarinic acid (CID: 5281792)	NP	NP	NP	-10.3
12	Chlorogenic acid (CID:1794427)	NP	-8.92	-9.04	-7.45
13	Theaflavine (CID: 135403798)	-9.74	-9.94	NP	NP
14	Aegelinol (CID: 600671)	NP	NP	NP	-7.95
15	Melanoxetin (CID: 15560442)	NP	NP	NP	-7.39
16	N-formimidoyl Thienamycine (CID: 5288621)	NP	NP	NP	-6.97

***NP;** Not potential

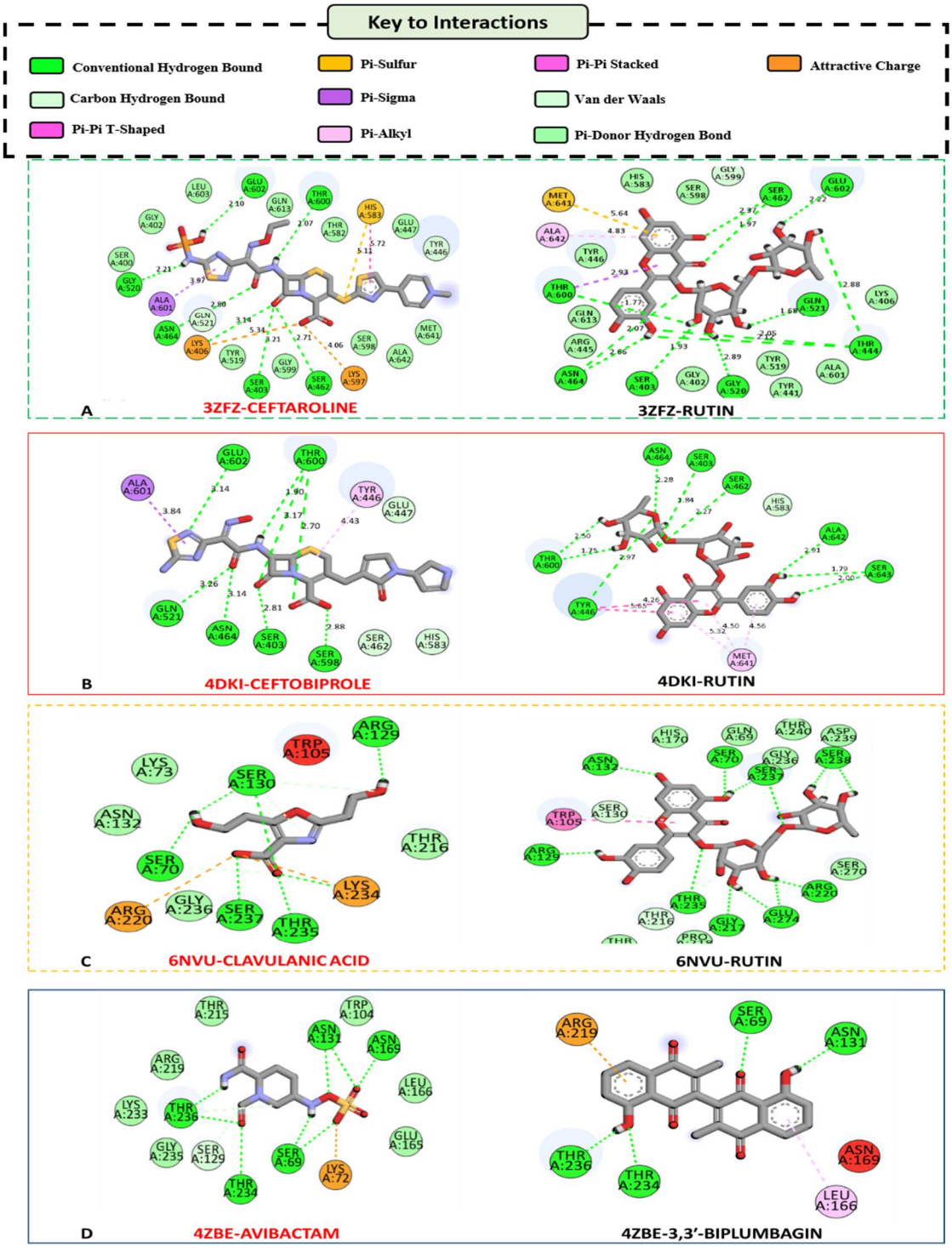

Figure 1 2D representation of ligand interactions in the active site pocket of **(A)** PBP2a, 3ZFZ; **(B)** PBP2a, 4DKI; (**C**) Beta-lactamase, 6NVU; **(D)** Beta-lactamase, 4ZBE

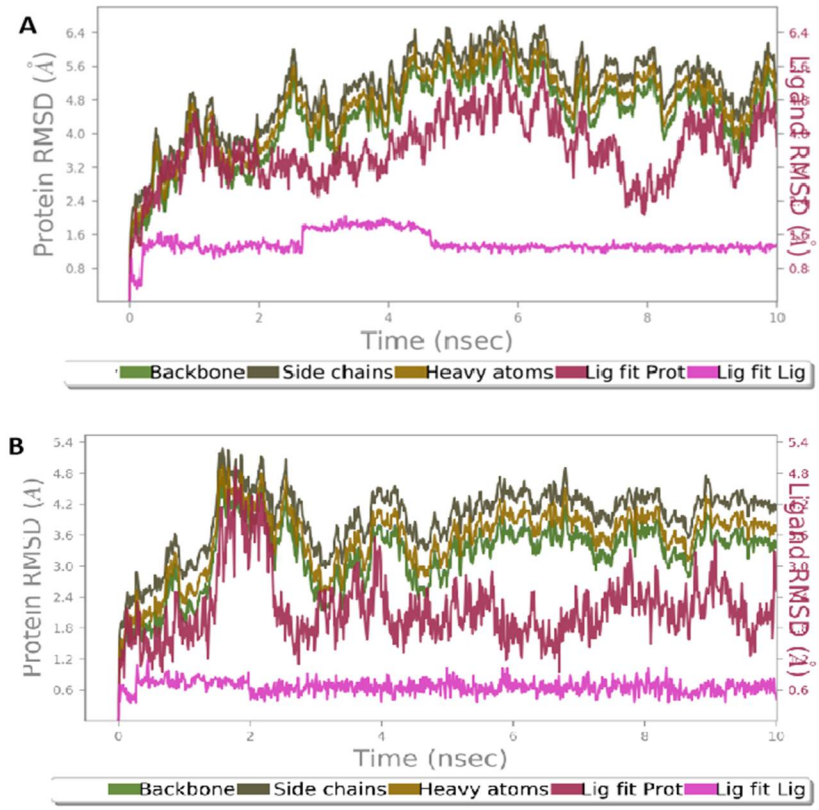

Figure 2 A 10 ns simulation profile of Protein-ligand interaction, root-mean-square deviation (RMSD) for **(A)** PBP2a-4DKI-Ceftobiprole and **(B)** PBP2a-4DKI-Rutin.

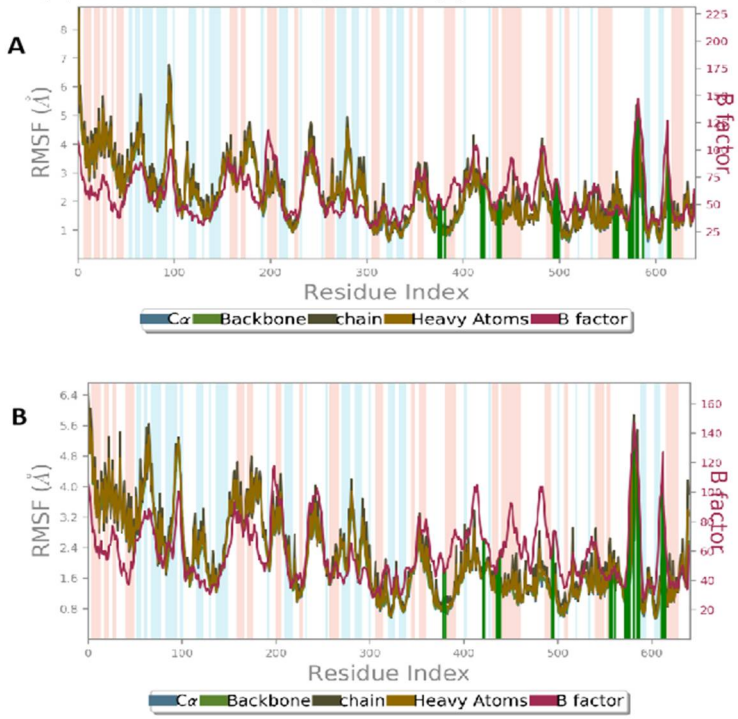

Figure 3 A 10 ns simulation profile of Protein-ligand interaction, root-mean-square fluctuation (RMSF) for **(A)** PBP2a-4DKI-Ceftobiprole and **(B)** PBP2a-4DKI-Rutin.

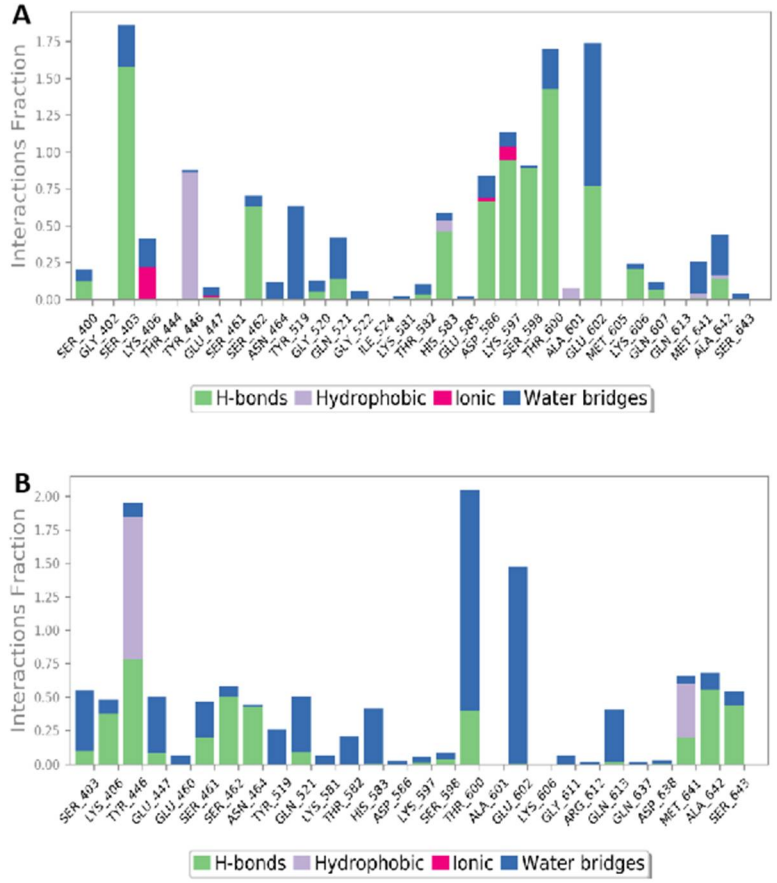

Figure 4 Interaction profile of crucial interacting amino acids of the PBP2a-4DKI in contact with **(A)** Ceftobiprole and **(B)** Rutin.

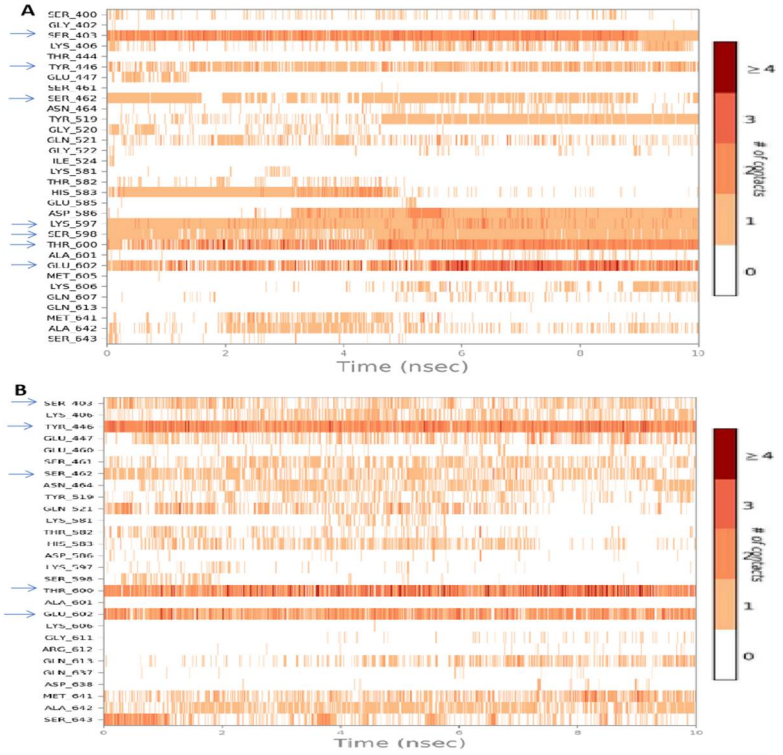

Figure 5 The timeline representation of the interactions of ligand with amino acids for the complex of **(A)** PBP2a-4DKI-Ceftobiprole and **(B)** PBP2a-4DKI-Rutin.

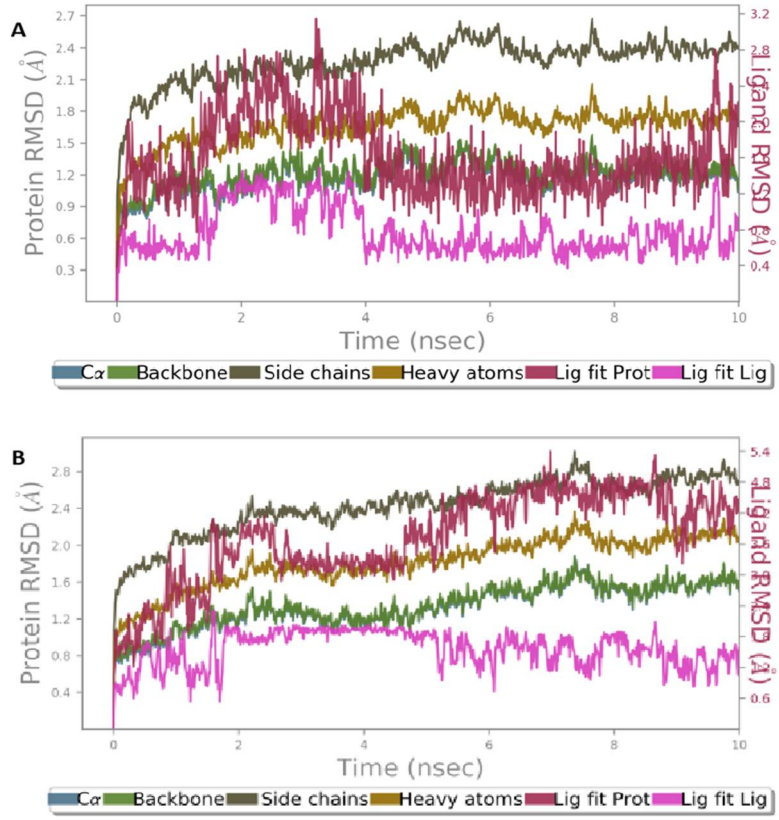

Figure 6 A 10 ns simulation profile of Protein-ligand interaction, root-mean-square deviation (RMSD) for **(A)** Beta-lactamase-6NVU-Clavulanic acid and **(B)** Beta-lactamase-6NVU-Rutin.

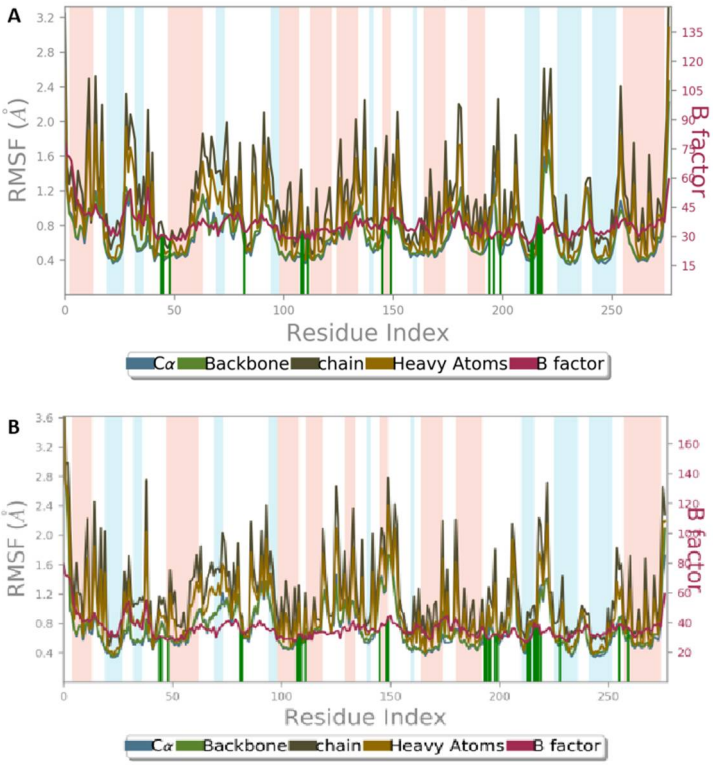

Figure 7 A 10 ns simulation profile of Protein-ligand interaction, root-mean-square fluctuation (RMSF) for **(A)** Beta-lactamase-6NVU-Clavulanic acid and **(B)** Beta-lactamase-6NVU-Rutin.

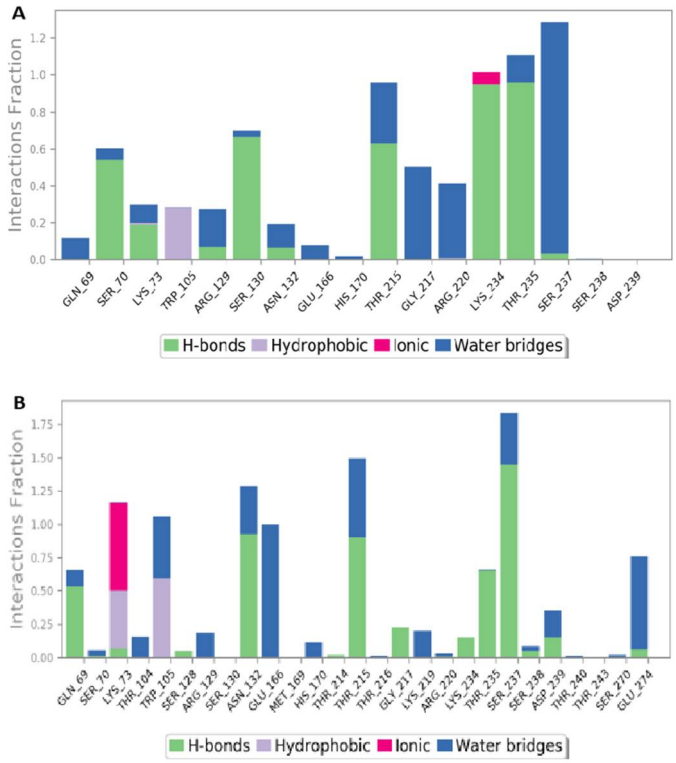

Figure 8 Interaction profile of crucial interacting amino acids of the Beta-lactamase-6NVU in contact with **(A)** Clavulanic acid and **(B)** Rutin.

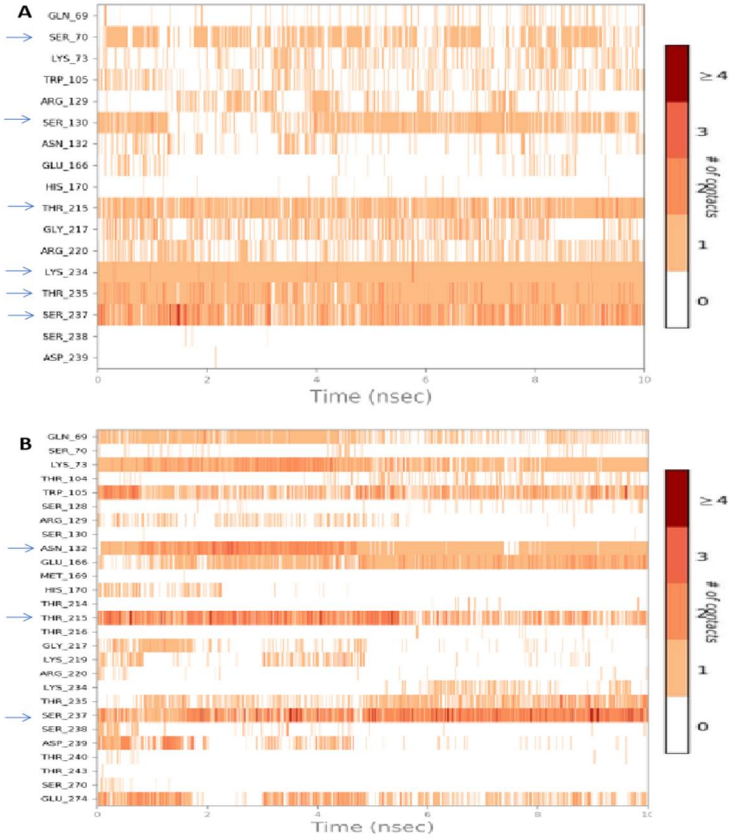

Figure 9 The timeline representation of the interactions of ligand with amino acids for the complex of **A)** Beta-lactamase-6NVU-Clavulanic acid and **(B)** Beta-lactamase-6NVU-Rutin.

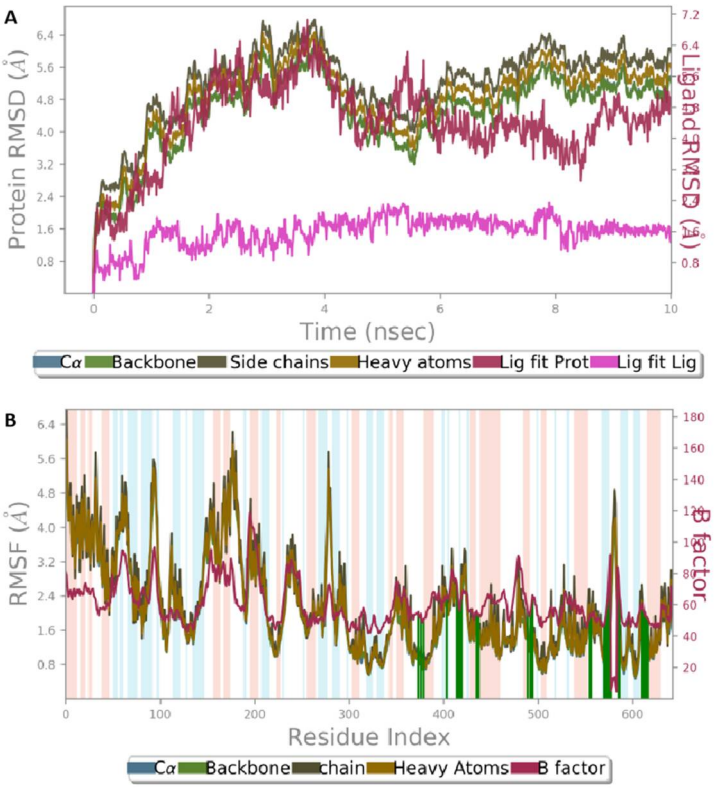

Figure 10 A 10 ns simulation profile of Protein-ligand interaction, **(A)** root-mean-square deviation (RMSD) and **(B)** root-mean-square fluctuation (RMSF) for PBP2a-3ZFZ-Rutin complex

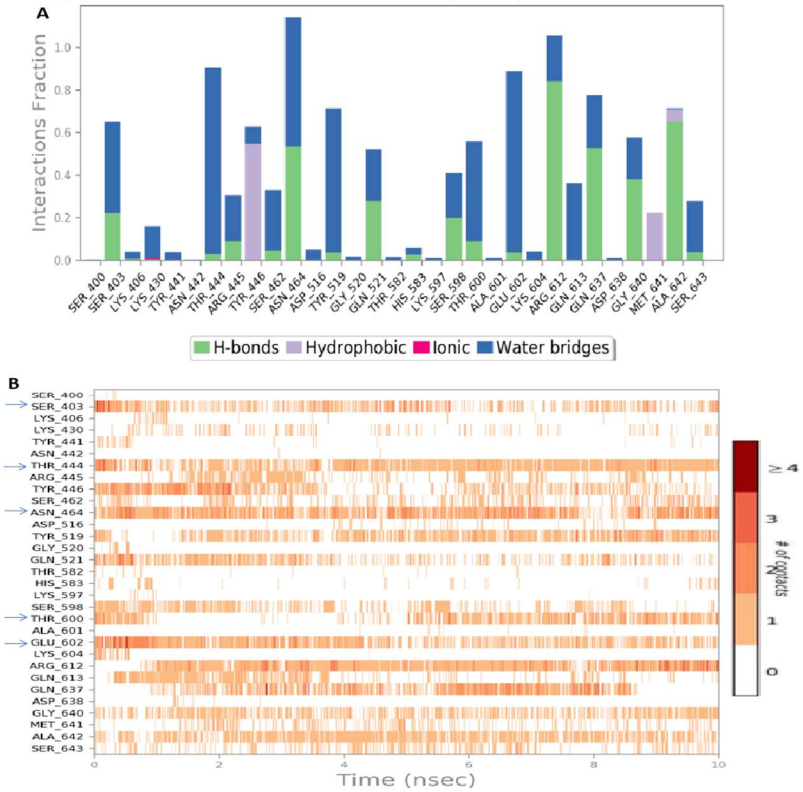

Figure 11 (A) Interaction profile of crucial interacting amino acids of the PBP2a-3ZFZ in contact with rutin. **(B)** The timeline representation of the interactions of ligand with amino acids for the complex of PBP2a-3ZFZ-Rutin.

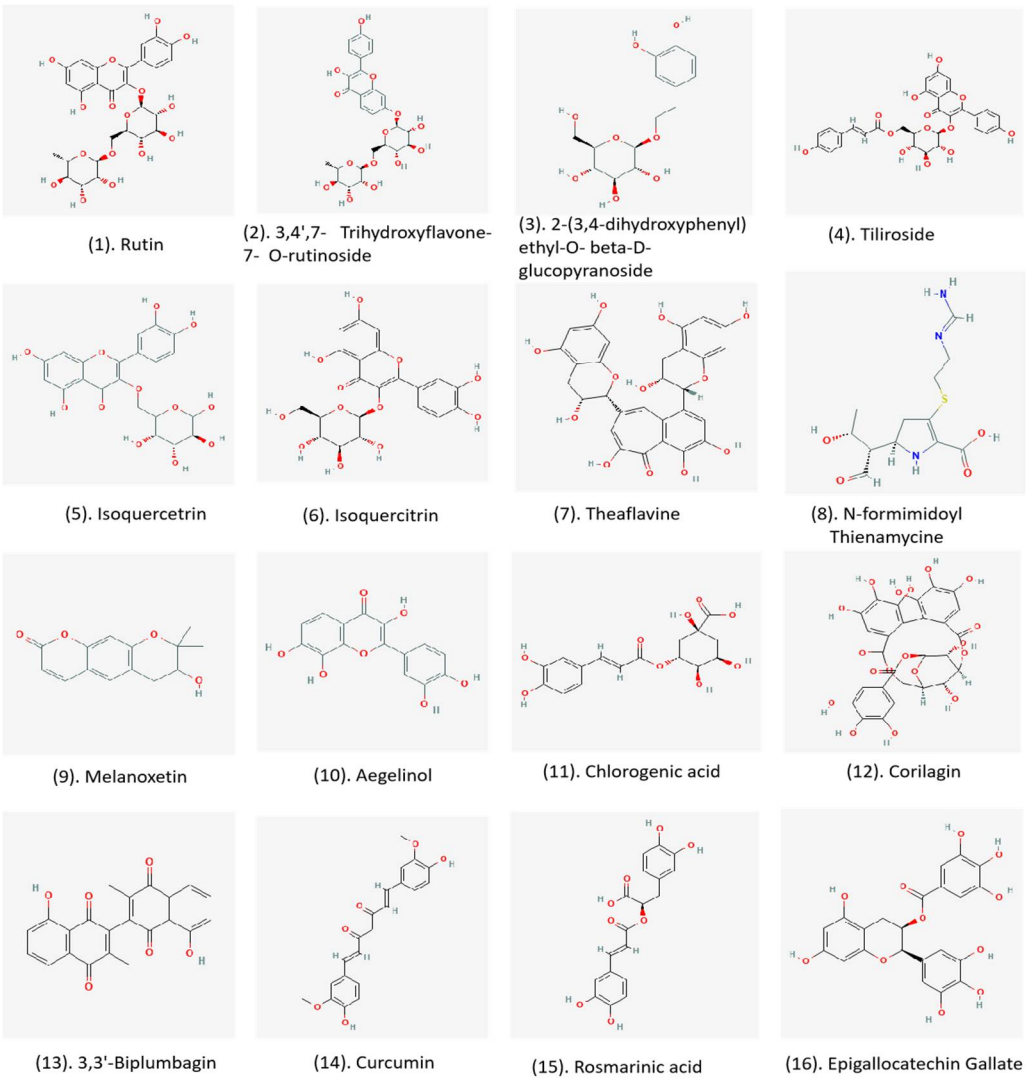

Figure 12 2D Structures of top 16 screened-out phytocompounds

DISCUSSION

Antibiotic resistance has continued to be a worldwide public health threat that keeps growing tremendously. Infectious bacteria that are resistant to beta-lactams such as methicillin resistant *Staphylococcus aureus* (MRSA), beta-lactamase producing bacteria; *E.coli* and *K. pneumoniae* are among the leading cause of bacterial infections worldwide (Christopher J L Murray et al.,2022). MRSA causes infections ranging from minor skin burn wound and skin infections to severe conditions such as infective endocarditis, staphylococcal scalded skin syndrome, and bacteraemia [13, 16, 47]. *E. coli* and *K. pneumoniae* are leading cause of urinary tract infections-(UTI), pneumonia, intra-abdominal infection, bloodstream infection (BSI), meningitis and pyogenic liver abscess (PLA) [48, 49]. MRSA has PBP2a enzyme with low binding affinity towards the beta-lactam antibiotics, *E. coli* and *K. pneumoniae* produce beta-lactamase enzymes that break open and hydrolyse beta-lactam ring of beta-lactam antibiotics. Hence, PBP2a and beta-lactamase plays a crucial role in the beta-lactam resistance. Due to their unusual enzymatic activity, beta-lactamase and PBP2a are considered as the prime target for beta-lactam resistance inhibitions. Development of inhibitors for PBP2a and beta-lactamases could reduce the rate of resistance as they are designed to inhibit the catalytic activity of the enzyme. Even though different inhibitors of PBP2a and beta-lactamases exist, they were reported to fail to act efficiently in blocking the enzyme activities, and have problems such as side effects and allergy, which necessitates identifying and designing novel inhibitors from natural products. Since natural products are considered safe, less or non-toxic, and cause less side effects.

In this present study natural plant products (phytocompounds) were selected and screened for the inhibition of PBP2a and beta-lactamase enzymes. A total of 16 top compounds (Figure 12) were screened out from a metadata of 553 phytocompounds and the analysed results are summarized in Tables 5.
On the basis of the Dock scores, rutin (**1**) was predicted as the top best ranked phytocompound to bind with the active site of MRSA's PBP2a, and beta-lactamase enzyme from *E. coli* while 3,3′-Biplumbagin (**13**) was predicted as the top best ranked phytocompound to bind with the active site of beta-lactamase enzyme from *K. pneumonia* (Figure 1). The strong interactions between PBP2a-rutin complexes were revealed by docking results with binding energy of -13.89 kcal mol^{-1} for PBP2a; 3ZFZ, with the formation of twelve (12) hydrogen bonds interaction, while the complex of PBP2a-ceftaroline has low binding energy (-8.65 kcal mol^{-1}) and formed less hydrogen bonds interaction (7 H-bonds) than that formed by rutin (Table 1). The complex of PBP2a; 4DKI-rutin, its stability was revealed by exhibiting higher binding energy of -12.6 kcal mol^{-1} greater than that of PBP2a; 4DKI-ceftobiprole complex with -8.9 kcal mol^{-1} and the formation of nine (9) hydrogen bonds interactions greater than that formed by ceftobiprole (8 H-bonds) (Table 2). In case of the beta-lactamases inhibition, beta-lactamase; 6NVU-rutin complex exhibited strong interaction of rutin to protein that was revealed by the docking binding energy of -10.54 kcal mol^{-1}, while the complex of beta-lactamase; 6NVU-clavulanic acid exhibited less binding energy of -6.2 kcal mol^{-1}. However, on the basis of hydrogen bonds formed, both rutin and clavulanic acid formed equal number of hydrogen bonds interaction (5 H-bonds) with *E. coli's* beta-lactamase binding site (Table 3). Furthermore, ranking of beta-lactamase; 4ZBE-3,3′-Biplumbagin complex as the top best inhibitor of beta-lactamase of *K. pneumoniae* was supported by the docking binding energy of -12.59 kcal mol^{-1} as compared to that of avibactam inhibitor of -6.7 kcal mol^{-1}). In case of hydrogen bonds interaction, 3,3′-Biplumbagin has less number of hydrogen bonds (4 H-bonds) as compared to that formed by reference avibactam (7 H-bonds) with *K. pneumoniae's* beta-lactamase binding site (Table 4).
In the previously published crystal structures of the MRSA's PBP2a; 3ZFZ-ceftaroline complex [42], MRSA's PBP2a; 4DKI-ceftobiprole complex [43], *E. coli* beta-lactamase; 6NVU-clavualnic acid complex [44] and *K. pneumoniae* beta-lactamase; 4ZBE-avibactam complex [45] provided the information about the interaction patterns of co-crystallized inhibitors and details of the key interacting amino acids of the active sites. Also, they suggested the significance of acylation between protein-ligand, and the significant amino acids involved in the acylation reaction between receptor site and ligand binding substituents. In which, for PBP2a they reported Ser403 as a key active site's amino acid that is responsible to form acylation reaction between its nucleophile and ligand (i.e. ceftaroline and ceftobiprole) in the binding pocket of the active sites. For beta-lactamase enzymes, they reported Ser70, and Ser237 as the key active site's amino acids involved in the interactions (acylation reactions) between receptor site and ligand (clavulanic acid) in the active site pocket of 6NVU. Furthermore, Ser69 in the active site of beta-lactamase; 4ZBE is responsible for the acylation reaction with avibactam inhibitor. Therefore, in consideration of that, it becomes necessary to observe analyze the interactions between key active site's residues and the docked ligands to understand the acylation interactions phenomenon which influences the inhibition of PBP2a and beta-lactamase enzymes. Finally, the results obtained from the docking process suggested that both rutin, 3,3′-biplumbagin, and reference ligands (ceftaroline, ceftobiprole, clavulanic acid and avibactam) formed hydrogen bonds interactions with the key amino acids in the active sites (i.e. Ser403 in PBP2a, Ser70, Ser237 and Ser69 in beta-lactamase enzymes).
Both rutin, ceftaroline, and ceftobiprole, each form one hydrogen bond interaction with key PBP2a active site's residue; Ser403, in which rutin interacted by a short H-bond with bond length 1.93 Å and ceftaroline interacted by H-bond with bond length 3.21 Å in the active site of 3ZFZ (Figure 1A). Also, rutin formed a short hydrogen bond with a bond length of 1.83 Å, and ceftobiprole formed a hydrogen bond with a bond length of 2.81 Å in the active site of 4DKI (Figure 1B). Rutin was the top best ligand against PBP2a; 4DKI, due to its higher binding energy, however, based on interacting residues, Isoquercetrin (**5**) (-11.91 kcal mol^{-1}) was the top ligand among the top 10 screened-out compounds by forming thirteen (13) hydrogen bonds interaction in the active site of 4DKI, of which three H-bonds were between key amino acid; Ser403, while rutin was the sixth ligand by forming nine (9) hydrogen bonds interaction with 4DKI of which, only one bond with Ser403 was formed (Table 2). Based on that, further analysis is needed to compare the interactions of rutin and Isoquercetrin with PBP2a, as the latter has the ability to form more hydrogen bonds in the active site of PBP2a than rutin. Moreover, Isoquercetrin exerted binding affinity (-11.91 kcal mol^{-1}) that is nearly equal to that of rutin (-12.6 kcal mol^{-1}). From the analysis of interacting key amino acids residues of beta-lactamase; 6NVU with clavulanic acid and rutin, it was observed that rutin formed only one hydrogen bond with Ser70 and two with Ser237 while clavulanic acid formed only one hydrogen bond between Ser70 and Ser237 in the active site. In addition, in the analysis of interacting amino acids residues of 6NVU with all the top 8 compounds it observed that hydrogen bonds formed by

phytocompounds were almost the same, whereby, most of the interactions were between Ser70, Ser237, Thr235, and Ser130, these findings were found to behave in consensus to the docking results of reference ligand (clavulanic acid) (Table 3), and to the previously reported interactions of clavulanic acid with 6NVU [44]. 3,3′-biplumbagin was found to interact with key Ser69 of beta-lactamase; 4ZBE, by forming one hydrogen bond interaction, while avibactam formed two hydrogen bonds with Ser69 (Table 4). Interestingly, rutin, the top best ligand against PBP2a and beta-lactamase; 6NVU, from *E.coli*, did not show good binding interaction with key amino acid; Ser69 of beta-lactamase; 4ZBE, though it exhibited high binding energy (-9.43 kcal mol^{-1}) to 4ZBE than avibactam (-6.7 kcal mol^{-1}) and with the ability to form nine (9) hydrogen bonds interaction.

CONCLUSION

The prepared metadata of 553 bioactive phytocompounds during this study contains the phytocompounds which were previously reported to have antimicrobial activity. However, the mechanisms of action for their antimicrobial activities are not known. Hence, the *in silico* analysis in this study has provided information on the mechanism of action of selected phytocompounds against beta-lactams resistant bacterial strains. The studied metadata showed the potentiality of phytocopmponds to act against MRSA and beta-lactamase producing bacteria, by having the ability to inhibit the bacteria through binding and blocking the resistant enzyme responsible for catalyzing the process of bacterial cell wall biosynthesis i.e. penicillin-binding protein 2a (PBP2a) and beta-lactamases. From the study results, it was observed that rutin and 3,3′-biplumbagin were capable to inhibit PBP2a and beta-lactamase by interacting with active site residues of the enzymes such as Ser403, Ser70, Ser237, and Ser69 which are considered as the key targeted amino acids in inhibiting the catalytic activity and function of PBP2a and beta-lactamases. Therefore, from the predicted mechanism of PBP2a and beta-lactamases inhibitions by phytocompounds particularly rutin and 3,3′-biplumbagin suggests that they have a higher potential to interact with the active site of PBP2a and beta-lactamase than the conventional reference inhibitors; ceftaroline, ceftobiprole, clavulanic acid, and avibactam, they may be considered as lead drug candidate for the development of new and effective drug molecules to treat beta-lactam resistant infections. Nevertheless, molecular dynamics and simulation and *in vitro* validation studies are of important to strengthen these *in silico* results, which are currently in process and planned to be communicated in the future.

ETHICAL APPROVAL

This article does not contain any studies with human participants or animals performed by any of the authors.

ACKNOWLEDGEMENTS

Author M.D., G.A.S, G.H.S and J..K.P acknowledges DST-FIST Sponsored Department of Microbiology and Biotechnology, School of Sciences, Gujarat University, for providing
necessary facilities to perform experiments.

COMPETING INTEREST

The authors have declared that no competing interest exists.

REFERENCES

1. Murray CJ, Ikuta KS, Sharara F, et al (2022) Global burden of bacterial antimicrobial resistance in 2019: a systematic analysis. Lancet 399:629–655. https://doi.org/10.1016/S0140-6736(21)02724-0
2. Khare T, Anand U, Dey A, et al (2021) Exploring Phytochemicals for Combating Antibiotic Resistance in Microbial Pathogens. Front Pharmacol 12:1–18. https://doi.org/10.3389/fphar.2021.720726
3. Reygaert WC (2018) An overview of the antimicrobial resistance mechanisms of bacteria. AIMS Microbiol 4:482–501. https://doi.org/10.3934/microbiol.2018.3.482
4. Lowy FD (2003) Antimicrobial resistance : the example of Staphylococcus aureus. 111:1265–1273. https://doi.org/10.1172/JCI200318535.In
5. Mahtab T, Jyoti A, Khusro A, et al (2021) Antibiotic resistance in microbes : History , mechanisms , therapeutic strategies and future prospects. J Infect Public Health 14:1750–1766. https://doi.org/10.1016/j.jiph.2021.10.020
6. Kirby WMM (1944) Extraction of a highly potent penicillin inactivator from penicillin resistant staphylococci. Science (80-) 99:452–453. https://doi.org/10.1126/science.99.2579.452
7. A. Bondi, Jr., C. C. Dietz PS (1945) Penicillin Resistant Staphylococci . Exp Biol Med 1945, 60 55 7–10
8. Chambers HF (1997) Methicillin Resistance in Staphylococci : Molecular and Biochemical Basis and Clinical Implications. Am Soc Microbiol 10:781–791
9. Chiang Y, Wong MTY, Essex JW (2020) Molecular Dynamics Simulations of Antibiotic Ceftaroline at the Allosteric Site of Penicillin-Binding Protein 2a (PBP2a). Isr J Chem 2020, 60, 754–763 754–763. https://doi.org/

10.1002/ijch.202000012
10. Sun S, Selmer M, Andersson DI (2014) Resistance to β-lactam antibiotics conferred by point mutations in penicillin-binding proteins PBP3, PBP4 and PBP6 in Salmonella enterica. PLoS One 9:1–10. https://doi.org/10.1371/journal.pone.0097202
11. Donald J. Tipper and Jack L., Strominger (1966) Mechanism Of Action Of Penicillins: A Proposal Based On Their Structural Similarity To Acyl-D-Alanyl-D-Alanine. Microbiology 54:. https://doi.org/10.1073/pnas.54.4.1133
12. Cochrane SA, Lohans CT (2020) Breaking down the cell wall: Strategies for antibiotic discovery targeting bacterial transpeptidases. Eur J Med Chem 112262. https://doi.org/10.1016/j.ejmech.2020.112262
13. Turner NA, Sharma-kuinkel BK, Maskarinec SA, et al (2020) Methicillin-resistant Staphylococcus aureus: an overview of basic and clinical research. Nature 17:203–218. https://doi.org/10.1038/s41579-018-0147-4.Methicillin-resistant
14. Kim C, Milheiriço C, Gardete S, et al (2012) Properties of a Novel PBP2A Protein Homolog from Staphylococcus aureus Strain LGA251 and Its Contribution to the Beta-Lactam-resistant Phenotype. J Biol Chem VOL 287:36854–36863. https://doi.org/10.1074/jbc.M112.395962
15. Maria G, Fabio R, Tommaso A (2016) Mechanisms of Antibacterial Resistance, Fourth Edi. Elsevier Ltd
16. Livermore DM (2000) Antibiotic resistance in staphylococci. Int J Antimicrob Agents 16:3–10. https://doi.org/https://doi.org/10.1016/s0924-8579(00)00299-5
17. Lim D, Strynadka NCJ (2002) Structural basis for the β-lactam resistance of PBP2a from methicillin-resistant Staphylococcus aureus. Nat Struct Biol 9:870–876. https://doi.org/10.1038/nsb858
18. Lima LM, Nascimento B, Barbosa G, Eliezer J (2020) β-Lactam antibiotics: An overview from a medicinal chemistry perspective. Eur J Med Chem 112829. https://doi.org/10.1016/j.ejmech.2020.112829
19. Tooke CL, Hinchliffe P, Bragginton EC, et al (2019) β-Lactamases and β-Lactamase Inhibitors in the 21st Century. J Mol Biol 431:3472–3500. https://doi.org/10.1016/j.jmb.2019.04.002
20. Khanna NR G V. (2022) Mechanism of Action. In: Beta Lactamase Inhibitor. Treasure Island (FL): StatPearls Publishing, pp 1–5
21. Nandhini P, Kumar P, Mickymaray S, et al (2022) Recent Developments in Methicillin-Resistant Staphylococcus aureus (MRSA) Treatment: A Review. Antibiotics 11:1–21. https://doi.org/10.3390/antibiotics11050606
22. Parham S, Kharazi AZ, Bakhsheshi-Rad HR, et al (2020) Antioxidant, antimicrobial and antiviral properties of herbal materials. Antioxidants 9:1–36. https://doi.org/10.3390/antiox9121309
23. Shedoeva A, Leavesley D, Upton Z, Fan C (2019) Wound healing and the use of medicinal plants. Evidence-based Complement Altern Med 2019:30. https://doi.org/10.1155/2019/2684108
24. Dattatray TV, Shivaji1 CS (2021) A comprehensive review of Polyalthia longifolia. Tradit Med Res 1–12. https://doi.org/10.12032/TMR20201218212
25. Shi Y, Zhang C, Li X (2021) Traditional medicine in India. J Tradit Chinese Med Sci 8:S51–S55. https://doi.org/10.1016/J.JTCMS.2020.06.007
26. Qian H, Zhang J, Zhao J (2022) How many known vascular plant species are there in the world? An integration of multiple global plant databases. Biodivers Sci 30:1–5. https://doi.org/10.17520/biods.2022254
27. Gurib-Fakim A (2006) Medicinal plants: Traditions of yesterday and drugs of tomorrow. Mol Aspects Med 27:1–93. https://doi.org/10.1016/J.MAM.2005.07.008
28. Chavan SS, Shamkuwar PB, Damale MG, Pawar DP (2014) A Comprehensive Review On Annona Reticulata. Int J Pharm Sci Res 5:45. https://doi.org/10.13040/IJPSR.0975-8232.5(1).45-50
29. Caesar LK, Cech NB (2019) Synergy and antagonism in natural product extracts: when 1 + 1 does not equal 2. Nat Prod Rep 36:869. https://doi.org/10.1039/C9NP00011A
30. Liang M, Ge X, Xua H, et al (2022) Phytochemicals with activity against methicillin-resistant Staphylococcus aureus. Phytomedicine 100:154073. https://doi.org/10.1016/J.PHYMED.2022.154073
31. Hammer KA, Carson CF, Rileya T V. (2012) Effects of Melaleuca alternifolia (tea tree) essential oil and the major monoterpene component terpinen-4-ol on the development of single- and multistep antibiotic resistance and antimicrobial susceptibility. Antimicrob Agents Chemother 56:909–915. https://doi.org/10.1128/AAC.05741-11
32. Goel M, Kalra R, Ponnan P, et al (2020) Inhibition of penicillin-binding protein 2a (PBP2a) in methicillin resistant Staphylococcus aureus (MRSA) by combination of oxacillin and a bioactive compound from Ramalinaroesleri Mayurika. Microb Pathog 104676. https://doi.org/10.1016/j.micpath.2020.104676
33. Maulana RU (2022) In-Silico Analysis of Active Compounds from Herbal Plants Against Penicillin Binding Protein 2a (PBP2a) of Methicillin-Resistant Staphylococcus Aureus. Res Sq 1–11
34. P.T.V. Lakshmi SR and AA (2011) Molecular Docking Analysisi of Phyto-Ligands with Multi Drug Resistant Beta-Lactamases of Stampylococcus aureusNo Title. Trends in Bioinfomatics 4:23–34. https://doi.org/10.3923/tb.2011.23.34
35. Mohamed SB, Adlan TA, Khalafalla NA, et al (2019) Proteomics and Docking Study Targeting Penicillin-Binding Protein and Penicillin-Binding Protein2a of Methicillin-Resistant Staphylococcus aureus Strain SO-1977 Isolated from Sudan. Evol Bioinforma 15:. https://doi.org/10.1177/1176934319864945
36. Santiago C, Pang EL, Lim KH, et al (2015) Inhibition of penicillin-binding protein 2a (PBP2a) in methicillin resistant Staphylococcus aureus (MRSA) by combination of ampicillin and a bioactive fraction from Duabanga grandiflora. BMC Complement Altern Med 15:1–7. https://doi.org/10.1186/s12906-015-0699-z
37. O'Boyle NM, Banck M, James CA, et al (2011) Open Babel. J Cheminform 3:1–14
38. Pettersen EF, Goddard TD, Huang CC, et al (2004) UCSF Chimera - A visualization system for exploratory research

and analysis. J Comput Chem 25:1605–1612. https://doi.org/10.1002/JCC.20084
39. Trott O, Olson AJ (2010) AutoDock Vina: improving the speed and accuracy of docking with a new scoring function, efficient optimization and multithreading. J Comput Chem 31:455. https://doi.org/10.1002/JCC.21334
40. Bowers KJ, Chow E, Xu H, et al (2006) Scalable algorithms for molecular dynamics simulations on commodity clusters. Proc 2006 ACM/IEEE Conf Supercomput SC'06. https://doi.org/10.1145/1188455.1188544
41. Parmar P, Rao P, Sharma A, et al (2022) Meticulous assessment of natural compounds from NPASS database for identifying analogue of GRL0617, the only known inhibitor for SARS - CoV2 papain-like protease (PLpro) using rigorous computational workflow. Mol Divers 26:389–407. https://doi.org/10.1007/s11030-021-10233-3
42. Otero LH, Rojas-altuve A, Llarrull LI, et al (2013) How allosteric control of Staphylococcus aureus penicillin binding protein 2a enables methicillin resistance and physiological function. PNAS 110:16808–16813. https://doi.org/10.1073/pnas.1300118110
43. Lovering AL, Gretes MC, Safadi SS, et al (2012) Structural insights into the anti-methicillin-resistant Staphylococcus aureus (MRSA) activity of ceftobiprole. J Biol Chem 287:32096–32102. https://doi.org/10.1074/jbc.M112.355644
44. Cifuentes-Castro V, Rodríguez-Almazán C, Silva-Sánchez J, Rudiño-Piñera E (2020) The crystal structure of ESBL TLA-1 in complex with clavulanic acid reveals a second acylation site. Biochem Biophys Res Commun 522:545–551. https://doi.org/10.1016/j.bbrc.2019.11.138
45. Krishnan NP, Nguyen NQ, Papp-Wallace KM, et al (2015) Inhibition of Klebsiella β-lactamases (SHV-1 and KPC-2) by avibactam: A structural study. PLoS One 10:1–13. https://doi.org/10.1371/journal.pone.0136813
46. Christopher J L Murray, Kevin Shunji Ikuta, Fablina Sharara, Lucien Swetschinski (2022) Articles Global burden of bacterial antimicrobial resistance in 2019 : a systematic analysis. Lancet 2022 399: 629–55. https://doi.org/10.1016/S0140-6736(21)02724-0
47. Tong SYC, Davis JS, Eichenberger E, et al (2015) Staphylococcus aureus Infections : Epidemiology , Pathophysiology , Clinical Manifestations , and Management. 28:603–661. https://doi.org/10.1128/CMR.00134-14
48. Hyun M, Lee JY, Kim H, Ryu SY (2019) Comparison of Escherichia coli and Klebsiella pneumoniae Acute Pyelonephritis in Korean Patients. Infect Chemother 51:130–141. https://doi.org/https://doi.org/10.3947%2Fic.2019.51.2.130
49. Kalin M, Giske CG, Vading M, Naucle P (2018) Invasive infection caused by Klebsiella pneumoniae is a disease affecting patients with high comorbidity and associated with high long-term mortality. PLoS One 13:1–13. https://doi.org/https://doi.org/10.1371/journal.pone.0195258